ICIC Express Letters
Volume **12**, Number **7**, July **2018**

 ISSN 1881-803X
pp. **707–713**

A NOVEL NON-LOCAL MEANS DESPECKLING ALGORITHM BASED ON TWO RATIO DISTANCES FOR SAR IMAGES

Xiaofei Shi[1], Jiande Feng[1], Derui Song[2,3], Tianshuang Qiu[4]
Min Zhang[1] and Li Li[5]

[1]Information Science and Technology College
Dalian Maritime University
No. 1, Linghai Road, Ganjingzi District, Dalian 116026, P. R. China
shi_xiao_fei_57@163.com

[2]School of Urban and Environmental Sciences
Liaoning Normal University
No. 850, Huanghe Road, Dalian 116029, P. R. China

[3]National Marine Environmental Monitoring Center
No. 42, Linghe Street, Shahekou District, Dalian 116023, P. R. China
drsong@nmemc.org.cn

[4]Faculty of Electronic Information and Electrical Engineering
Dalian University of Technology
No. 2, Linggong Road, Ganjingzi District, Dalian 116024, P. R. China
qiutsh@dlut.edu.cn

[5]Information Engineering College
Dalian University
No. 10, Xuefu Street, Economic and Technological Development Zone, Dalian 116622, P. R. China
ffsimplemsu@gmail.com

Received November 2017; accepted February 2018

Abstract. *Non-local means (NLM) algorithms are of importance in despeckling for synthetic aperture radar (SAR) images. Pixel-relativity measurement based NLM algorithm is a popular one, which uses eight directions in a search window, to search for homogeneous regions as a key step. Such approach may not guarantee to obtain homogenous region accurately in patches with complicated textures and sharp borders, due to depending on the limited directions. In this paper, a novel NLM algorithm based on two ratio distances is proposed, without need to obtain homogeneous regions, to reduce speckles of patches. The first similarity measurement is based on ratio distance of two intensity patches, with the minimized ratio distance value to demonstrate the maximum similarity, utilizing intensity similarity that is more straight than that of existing pixel-relativity based method, which is dependent on the probability density function of two patches in local homogeneous region. Then such ratio distance is proved valid for SAR images. To keep good precision of similarity at borders, second ratio distance with central pixel value of patches is presented, followed with the space location distance to reduce the effect of the farthest patches to current patch. Applying to SAR images, experimental results show that the proposed NLM algorithm has better performance than some of existing despeckling algorithms, especially in despeckling ability.*
Keywords: NLM, Despeckling, SAR, Ratio distance, Similarity

1. **Introduction.** Due to the all-day, all-weather acquisition capability, synthetic aperture radar (SAR) images offer more advantages over optical images [1]. However, the main problem is the presence of speckle, which degrades the visual appearance and detailed extraction of SAR images and poses strong hindrances to high-level tasks, such

DOI: 10.24507/icicel.12.07.707

as classification, target detection and tracking. Therefore, despeckling [2] is a fundamental and crucial preprocessing step for SAR images processing. Classic techniques on despeckling are deployed in the spatial domain and are obtained by making assumptions on the statistical properties of reflectivity and speckle, such as Lee filter [3], Frost filter [4], Kuan filter [5] and MAP filter [6]. Some other methods have also been proposed for obtaining better speckle reduction such as partial differential equation method [7-9], subspace method [10], transform-based method [11], neural network method [12] and sparse representation method [13].

In recent years, non-local means (NLM) [14] has attracted more interests in image processing. By exploiting image self similarity, nonlocal filtering mimics a true statistical averaging of pixels, thus allowing strong speckle reduction and good preservation of features. However, the first NLM filtering method proposed to handle additive noise is not valid for speckle [15]. To SAR images de-speckling, SAR-BM3D [16] combines local filtering and wavelet-domain shrinkage, in which a probabilistic similarity is utilized for patch-matching. [17] uses Euclidean distance and coefficient variation to adjust the decay parameters to complete despeckling. To reduce calculation burden, [18] exploits activity level in each patch to drive search zone, and a probabilistic termination approach and look-up table are utilized to speed up patch matching and processing expense. A probabilistic non-local weight based despeckling algorithm uses guided filtering in the Bayesian non-local framework [19], in which normalization coefficients are derived from image statistics. PPB [20] uses maximum likelihood estimation to provide iteratively refined despeckling.

The aim of this paper is to propose a novel NLM algorithm with two ratio distances, inspired by [15], but without need to determine homogeneous region that has to be conducted with a search window prior to despeckling in [15], because the homogeneity of search window in [15] is a question merely with limited directions. This means that all pixels in search window obtained from [15] could not always keep homogeneous due to complicated textures and borders in SAR images. In this paper, a new ratio distance of two pixels patches is proposed, which is used to measure the similarity of two patches that have no restrictions on the homogeneity. To keep good precision of similarity at borders, second similarity criterion with central pixel value is presented, followed with a space location distance to reduce influence of the farthest patches on current one. The proposed NLM algorithm can demonstrate better performance in SAR images, especially in despeckling aspect, in contrast with some existing despeckling algorithms.

The rest of this paper is organized as follows. Section 2 gives an explanation of the proposed algorithm in detail. Section 3 presents the experimental results and evaluates the performance of the proposed algorithm in SAR images. Finally, we summarize this paper in Section 4.

2. Description of the Proposed NLM Algorithm.

2.1. **Two novel ratio distances.** [15] utilizes a probability density function of ratio, which has to obtain the homogeneous region in search window. While such a search window with eight directions cannot be guaranteed to be homogeneous due to the complexity of texture and borders in SAR images. To solve this problem, we propose a ratio distance D_P to measure the similarity of two patches by pixel values and D_P is defined as

$$D_P = \left| \max \left\{ \left\| Y_{N_i} \cdot \diagup Y_{N_j} \right\|_2^2, \left\| Y_{N_j} \cdot \diagup Y_{N_i} \right\|_2^2 \right\} - M \right| \tag{1}$$

where N_i and N_j denote the numbers of two patches; Y_{N_i} and Y_{N_j} denote the pixel values in patches N_i and N_j. The symbol of $\cdot\diagup$ denotes the dot quotient of two vectors and M denotes the number of pixels in image patches f_{N_i} and f_{N_j}. $\|\cdot\|_2$ represents Euclidean norm and $|\cdot|$ is absolute value operator. It can be seen from (1) that D_P is closer to zero

with larger similarity between two patches, while farther from zero with less similarity. The expectation of (1) has been theoretically verified to preserve the similarity of two patches of SAR images robustly, wherever noise image patches N_i and N_j are in the uniform or heterogeneous regions. It could be seen that (1) can be rewritten as

$$D_p = \left| \max \left\{ \sum_{k=1}^{M} \left| \frac{Y_{N_i}(k)}{Y_{N_j}(k)} \right|^2, \sum_{k=1}^{M} \left| \frac{Y_{N_j}(k)}{Y_{N_i}(k)} \right|^2 \right\} - \sum_{k=1}^{M} 1^2 \right| \tag{2}$$

To strengthen the role of the central pixel value and its nearest neighbor in two patches, a standard Gaussian kernel G is introduced into (2), where G must obey $\sum_{k=1}^{M} G(k) = 1$, and we obtain

$$D_p = \left| \max \left\{ \sum_{k=1}^{M} G(k) \left| \frac{Y_{N_i}(k)}{Y_{N_j}(k)} \right|^2, \sum_{k=1}^{M} G(k) \left| \frac{Y_{N_j}(k)}{Y_{N_i}(k)} \right|^2 \right\} - \sum_{k=1}^{M} G(k) \right| \tag{3}$$

Due to the integral of standard Gaussian kernel being one, (3) can be described by

$$D_p = \left| \max \left\{ \sum_{k=1}^{M} G(k) \left| \frac{Y_{N_i}(k)}{Y_{N_j}(k)} \right|^2, \sum_{k=1}^{M} G(k) \left| \frac{Y_{N_j}(k)}{Y_{N_i}(k)} \right|^2 \right\} - 1 \right| \tag{4}$$

In order to increase the precision of similarity of the proposed NLM algorithm in border, we present another ratio distance D_B to make up the drawback of (4). D_B is defined as

$$D_B = \left| \max \left(\frac{Y_{N_i}(i)}{Y_{N_j}(j)}, \frac{Y_{N_j}(i)}{Y_{N_i}(j)} \right) - 1 \right| \tag{5}$$

where i and j stand for the central locations in patches N_i and N_j. If two patches locate in the same homogeneous region, D_B will be small. If two patches are in two different regions, D_B will be larger due to the large difference in central pixel value for two patches. From (4), a standard Gaussian kernel is utilized to consider space location of all pixel values in each patch, which is used to strengthen the role of central pixel and nearby in each patch in an inner-patches manner. Space location of inter-patches has never been treated as a problem. It is well known that the neighboring patches play more significant role on current patch than that of the farthest patches. To attain this goal, similar to Gaussian kernel idea, we construct a space location distance for inter-patches that is defined as $D_S(i, j)$, where i and j stand for the central locations in patches N_i and N_j mentioned above, and $D_S(i, j)$ is the Euclidean distance between i and j.

2.2. **Proposed NLM algorithm with two ratio distances.** In this section, we design the proposed NLM algorithm with two ratio distances mentioned above. Similar to [21], we evaluate the pixel value by

$$NLMSAR_I(i) = \sum_j w(i, j) I(j) \tag{6}$$

where $I(j)$ represents the pixel value in location of j, and $w(i, j)$ is described by

$$w(i, j) = \frac{1}{Z(i)} \left\{ \exp\left(-\frac{D_P}{h_1^2} \right) * \exp\left(-\frac{D_B}{h_2^2} \right) * \exp\left(-\frac{D_S}{h_3^2} \right) \right\} \tag{7}$$

where h_1, h_2 and h_3 are the decay control parameters and we set $h_1 = h_2 = h_3 = kL\sigma$, where k is a constant, with L representing the number of looks in an SAR image, and σ representing the standard deviation. $Z(i)$ is a normalization factor and can be described by

$$Z(i) = \sum_j \left\{ \exp\left(-\frac{D_P}{h_1^2} \right) * \exp\left(-\frac{D_B}{h_2^2} \right) * \exp\left(-\frac{D_S}{h_3^2} \right) \right\} \tag{8}$$

The whole process of the proposed NLM algorithm could be described as a flowchart in Figure 1. Initially, we started with an SAR image. Then the sizes of two windows,

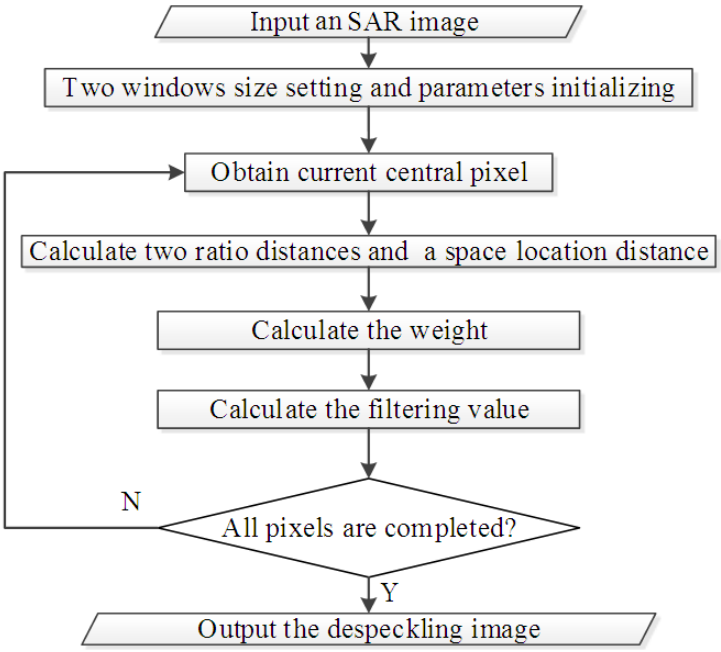

FIGURE 1. The flowchart of the proposed NLM algorithm

searching window and patches, need to be constant and we set the initial values for h_1, h_2 and h_3. We select a pixel from the SAR image as current central pixel and calculate D_P, D_B and D_S. Then the weight in (7) is calculated. The evaluated pixel is obtained by (6). The despeckling SAR image will be outputted if all pixels in original image have been filtered.

3. **Experimental Results and Discussion.** In order to quantitatively evaluate the performance of the proposed method, two evaluation criteria are introduced. *ENL* measures the degree of speckle reduction in a homogeneous region, which is given by [22]. In practice, we should artificially choose the homogeneous region to be as large as possible. A large *ENL* value corresponds to better speckle suppression. *EPD-ROA* reveals the ability of edge preservation, which is defined by [15]. A larger *EPD-ROA* value corresponds to better feature preservation. Four real SAR images are tested. Visual and numerical results are obtained for these images. The results of our approach (Non-local means with two ratio distances, named NLM-TRD) for these real SAR images are compared with those of SAR-BM3D [16], Frost filter [4], SRAD [9], and PPB [20]. For the proposed NLM-TRD algorithm, the sizes of search window and similarity patch are 21×21 and 7×7, respectively. The sizes of sliding window in Frost filter is 7×7. The size of sliding window in SRAD is 3×3, and step size is set as 0.1 with iteration number by 80. We use default parameters of SAR-BM3D in [16].

3.1. **Experimental results for real SAR images.** In Figure 2, experimental results are demonstrated with five algorithms. (a) is a real SAR image. The images in (b), (c), (d), (e) and (f) are despeckling results of Frost, SRAD, SAR-BM3D, PPB and the proposed NLM-TRD. Frost and SRAD are widely used in the community, but they provide only a limited speckle suppression if compared with nonlocal filters in general, and with the proposed approach. SAR-BM3D is found to retain residuals of speckle in homogeneous regions and this is evident in visual analysis. The proposed NLM-TRD is similar to PPB, both of which can suppress the speckle better than other three algorithms, while a bit weak in feature preservation versus SAR-BM3D.

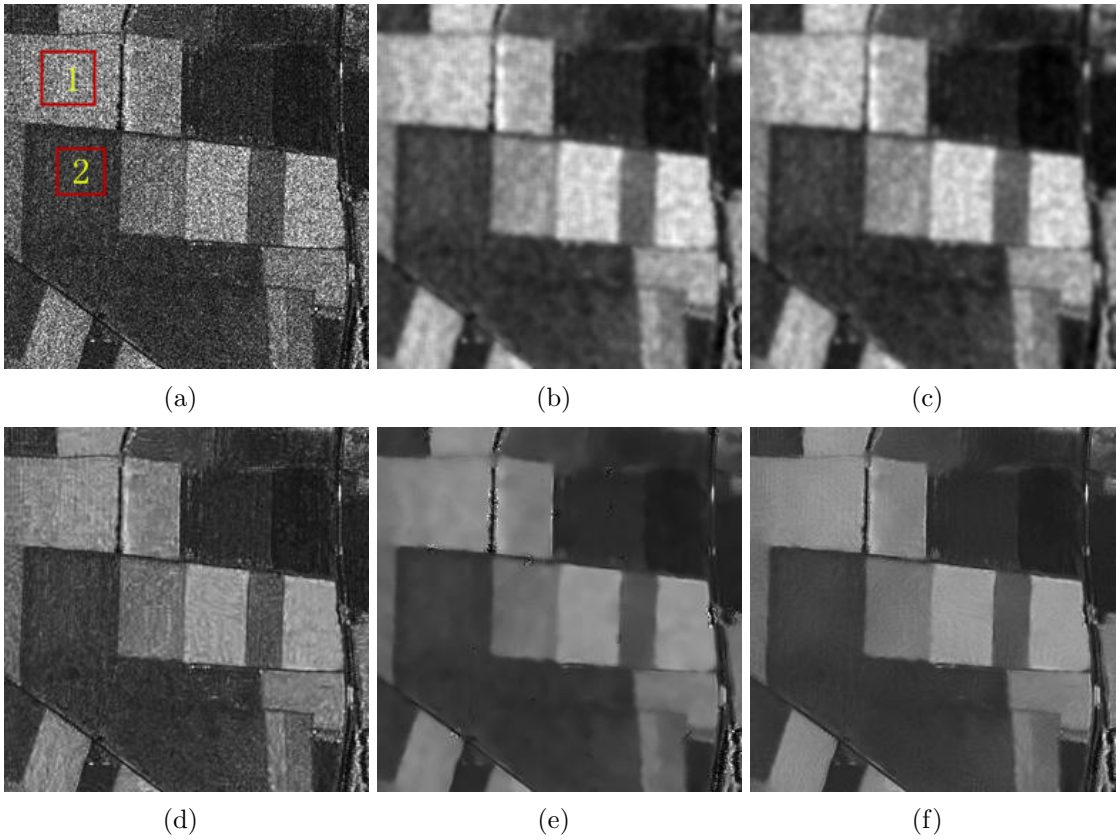

FIGURE 2. Despeckling results on one real SAR image from four images: (a) original SAR image, (b) result of frost, (c) result of SRAD, (d) result of SAR-BM3D, (e) result of PPB and (f) result of NLM-TRD proposed in this paper

TABLE 1. *ENL* and *EPD-ROA* for the first SAR image

	ENL		*EPD-ROA*	
	Zone 1	Zone 2	HD	VD
Frost	67.9858	65.4090	0.2297	0.0594
SRAD	80.8264	82.7867	0.1979	0.0390
SAR-BM3D	31.4246	13.0774	0.4841	0.2289
PPB	175.8216	134.3267	0.4206	0.1315
NLM-TRD	170.1871	180.6763	0.3661	0.1343

TABLE 2. *ENL* and *EPD-ROA* for the second SAR image

	ENL		*EPD-ROA*	
	Zone 1	Zone 2	HD	VD
Frost	48.2437	75.0610	0.1550	0.1158
SRAD	62.1756	78.8367	0.1308	0.0968
SAR-BM3D	29.5581	23.9532	0.3580	0.3298
PPB	130.2001	68.3314	0.2766	0.2564
NLM-TRD	153.8291	152.3550	0.1668	0.1327

TABLE 3. *ENL* and *EPD-ROA* for the third SAR image

	ENL		*EPD-ROA*	
	Zone 1	Zone 2	HD	VD
Frost	106.3116	153.1039	0.2843	0.0831
SRAD	80.8264	209.0098	0.2672	0.0625
SAR-BM3D	20.5972	33.2538	0.4926	0.2334
PPB	169.1181	382.9652	0.4867	0.1997
NLM-TRD	312.8022	770.0357	0.4023	0.2179

TABLE 4. *ENL* and *EPD-ROA* for the fourth SAR image

	ENL		*EPD-ROA*	
	Zone 1	Zone 2	HD	VD
Frost	109.9141	271.1901	0.1603	0.1896
SRAD	138.1085	333.7097	0.1545	0.1747
SAR-BM3D	21.1798	127.1209	0.4259	0.4540
PPB	256.6325	563.1561	0.3266	0.3674
NLM-TRD	356.1723	738.8549	0.2545	0.3038

3.2. **Performance comparison.** To evaluate the performance of above five algorithms, *ENL* and *EPD-ROA* are used for performance test, which are depicted in Table 1 to Table 4. *ENL* is calculated for the region marked by rectangle as shown in Figure 2(a) for all tested images. Two rectangle regions are selected and we name them as Zone 1 and Zone 2. From Table 1 to Table 4, HD and VD denote the horizontal and vertical directions, respectively, which are utilized to calculate the quantities in *EPD-ROA*. From Table 1 to Table 4, we can find generally, *ENL* in the proposed NLM-TRD demonstrates to be the largest, followed by PPB, SRAD, Frost, and SAR-BM3D, except that value of Zone 1 in Table 1, where *ENL* in PPB is larger than that in NLM-TRD. The difference between them in *ENL* is about 5.6, which does not mean PPB is better than NLM-TRD. The reason is that Zone 1 demonstrates a bit less homogeneity, and the standard deviation of PPB will be smaller than that of NLM-TRD. Therefore, the ENL in PPB is larger than that in NLM-TRD. From Table 1 to Table 4, the proposed NLM algorithm has the best despeckling ability in contrast with the other four algorithms. From Table 1 to Table 4, *EPD-ROA* in SAR-BM3D has the best performance, traced by PPB, the proposed NLM-TRD, Frost and SRAD. It means SAR-BM3D has the best feature preservation ability. NLM-TRD is weak in NLM algorithms but superior to non-NLM algorithms such as Frost and SRAD.

4. **Conclusions.** A novel despeckling algorithm with two ratio distances is proposed. The first pixels similarity measurement of patches is utilized to calculate the local means without need to determine the homogeneity. The second ratio distance is proposed to increase the precision of pixel evaluation at or near borders, companying with the space location distance to reduce the influence of the farthest patches to current one. Four real SAR images are utilized and experimental results demonstrate the good performance of the proposed NLM algorithm versus some existing despeckling algorithms, especially in despeckling ability. Future research will focus on feature preserving-based nonlocal despeckling and on the extension to the case of heavy tailed speckle.

Acknowledgment. This work is supported by the fund of Key Laboratory of Marine Management Technology in State Oceanic Administration People's Republic of China under Grant 201504, and partially supported by the National Natural Science Foundation

of China under Grant 61401055 and the Ph.D Programs Foundation of Liaoning Province of China 20170520421. The authors also gratefully acknowledge the helpful comments and suggestions of the reviewers, which have improved the presentation.

REFERENCES

[1] A. Moreira, P. Prats-Iraola, M. Younis, G. Krieger, I. Hajnsek and K. P. Papathanassiou, A tutorial on synthetic aperture radar, *IEEE Geoscience Remote Sensing Magazine*, vol.1, no.1, pp.6-43, 2013.

[2] S. Guo, Q. Wang, L. Wang and H. Zhu, Speckle noise reduction in ultrasonic images based on tensor voting, *ICIC Express Letters*, vol.8, no.11, pp.3185-3190, 2014.

[3] J. S. Lee, Digital image enhancement and noise filtering by use of local statistics, *IEEE Trans. Pattern Analysis and Machine Intelligence*, vol.PAMI-2, no.2, pp.165-168, 1980.

[4] V. S. Frost, J. A. Stiles, K. S. Shanmugan and J. C. Holtzman, A model for radar images and its application to adaptive digital filtering of multiplicative noise, *IEEE Trans. Pattern Analysis and Machine Intelligence*, vol.PAMI-4, no.2, pp.157-166, 1982.

[5] D. T. Kuan, A. A. Sawchuk, T. C. Strand and P. Chavel, Adaptive noise smoothing filter for images with signal-dependent noise, *IEEE Trans. Pattern Analysis and Machine Intelligence*, vol.PAMI-7, no.2, pp.165-177, 1985.

[6] A. Lopès, E. Nezry, R. Touzi and H. Laur, Structure detection and statistical adaptive speckle filtering in SAR images, *International Journal of Remote Sensing*, vol.14, no.9, pp.1735-1758, 1993.

[7] Z. L. Wang, X. T. Tan, Q. Yu and J. B. Zhu, Sparse PDE for SAR image speckle suppression, *IET Image Processing*, vol.11, no.6, pp.425-432, 2017.

[8] M. Zhang, Z. Yang and L. Ma, An adaptive image denoising method based on anisotropic diffusion equation, *ICIC Express Letters*, vol.6, no.7, pp.1877-1882, 2012.

[9] Y. G. Yu and S. T. Acton, Speckle reducing anisotropic diffusion, *IEEE Trans. Image Processing*, vol.11, no.11, pp.1260-1270, 2002.

[10] N. Yahya, N. S. Kamel and A. S. Malik, Subspace-based technique for speckle noise reduction in SAR images, *IEEE Trans. Geoscience and Remote Sensing*, vol.52, no.10, pp.6257-6271, 2014.

[11] F. Gao, X. S. Xue, J. P. Sun, J. Wang and Y. Zhang, A SAR image despeckling method based on two-dimensional S transform shrinkage, *IEEE Trans. Geoscience and Remote Sensing*, vol.54, no.5, pp.3025-3034, 2016.

[12] P. Y. Wang, H. Zhang and V. M. Patel, SAR image despeckling using a convolutional neural network, *IEEE Signal Processing Letters*, vol.24, no.12, pp.1763-1767, 2017.

[13] C. Ozcan, B. Sen and F. Nar, Sparsity-driven despeckling for SAR images, *IEEE Geoscience and Remote Sensing Letters*, vol.13, no.1, pp.115-119, 2016.

[14] A. Buades and B. Coll, A non-local algorithm for image denoising, *IEEE Computer Society Conference on Computer Vision and Pattern Recognition*, San Diego, USA, pp.60-65, 2005.

[15] H. X. Feng, B. Hou and M. G. Gong, SAR image despeckling based on local homogeneous-region segmentation by using pixel-relativity measurement, *IEEE Trans. Geoscience and Remote Sensing*, vol.49, no.7, pp.2724-2737, 2011.

[16] S. Parrilli, M. Poderico, C. V. Angelino and L. Verdoliva, A nonlocal SAR image denoising algorithm based on LLMMSE wavelet shrinkage, *IEEE Trans. Geoscience and Remote Sensing*, vol.50, no.2, pp.606-616, 2012.

[17] S. B. Chen, J. H. Hou, H. Zhang and B. Y. Da, De-speckling method based on non-local means and coefficient variation of SAR image, *Electronic Letters*, vol.50, no.18, pp.1314-1316, 2014.

[18] D. Cozzolino, S. Parrilli, G. Scarpa, G. Poggi and L. Verdoliva, Fast adaptive nonlocal SAR despeckling, *IEEE Geoscience and Remote Sensing Letters*, vol.11, no.2, pp.524-528, 2014.

[19] J. Gokul, M. S. Nair and J. Rajan, Guided SAR image despeckling with probabilistic non local weights, *Computer and Geosciences*, vol.109, pp.16-24, 2017.

[20] C. A. Deledalle, L. Denis and F. Tupin, Iterative weighted maximum likelihood denoising with probabilistic patch-based weights, *IEEE Trans. Image Processing*, vol.18, no.12, pp.2661-2672, 2009.

[21] H. Y. Zhao, Q. Wang and W. W. Wu, SAR image despeckling based on improved non-local means algorithm, *International Conference on Electromagnetics in Advanced Applications*, Palm Beach, pp.844-847, 2014.

[22] H. Xie, L. E. Pierce and F. T. Ulaby, SAR speckle reduction using wavelet denoising and Markov random field modeling, *IEEE Trans. Geoscience and Remote Sensing*, vol.40, no.11, pp.2196-2212, 2002.